Technical Meeting on Compatibility Between Coolants and Materials for Fusion Facilities and Advanced Fission Reactors
IAEA Headquarters Vienna, Austria and virtual participation via Cisco Webex 30 October–3 November 2023

MECHANISM OF THE LOCAL CORROSION OF FUEL ELEMENT CLADDING DUE TO DECOMPOSITION OF HYDROGEN SOLUTION IN THE NEIGHBORHOOD OF THE COOLANT SATURATION TEMPERATURE

A.S. IVANOV, P.A. KALASHNIKOVA, A.A. KOVALISHIN, M.D. TARAN
NRC "Kurchatov Institute",
Russia, Moscow

Introduction

A white deposit was observed on zirconium claddings of VVER-1000 fuel elements used in the development efforts for increasing the thermal power to 104 % of N_{nom} and in the implementation of the 18-months fuel cycle. Post-irradiation examination of the fuel assemblies (FA) showed that the white deposit was ZrO_2 oxide film up to 30 µm thick. The white deposit can be seen on almost all fuel elements in the peripheral and inner rows (see Figure 1). For the majority of fuel elements the white deposit starts either after the 12th spacer grid (12SG) or under the 12SG.

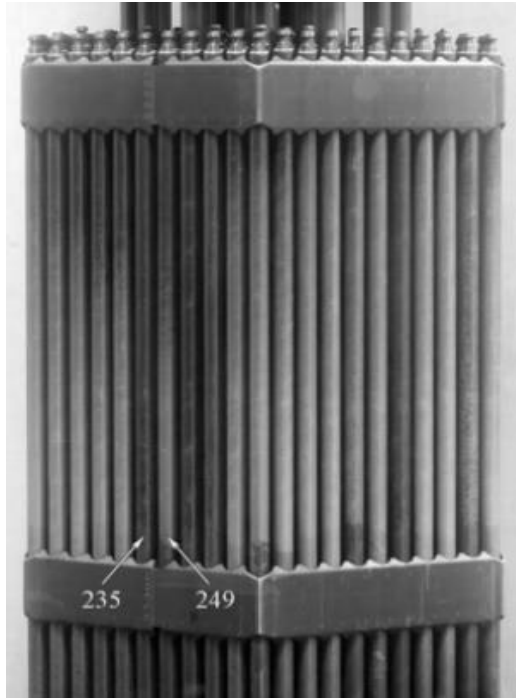# A white deposit on zirconium claddings of VVER-1000 fuel elements

Figure 1 – Appearance of FA fuel elements between the 12SG and 13SG [1]

[1] Volkova I.N., Goriachev A.V., Zvir E.A., Zhitelev V.A., Nikitin O.N., Strozhuk A.V., Results of Studying the Oxide Film Structure in High Oxidation Areas of Claddings of the TVS-2M Fuel Element after Operation in Unit 4 of the Balakovo NPP during One Fuel Campaign, The Eleventh International Science and Technology Conference ISTC2018, Moscow, Russia. http://mntk.rosenergoatom.ru/mediafiles/u/files/2018/MNTK_2018_Trudy_Color_small.pdf

New corrosion mechanisms

According to the analysis results, there are no deviations of monitored quality parameters of the primary circuit coolant from the allowed value ranges or deviations of diagnostic parameters from reference levels.

Despite the absence of deviations of monitored quality parameters of the primary circuit coolant from the allowed value ranges, essentially deeper corrosion of fuel element claddings is observed.

This may point to involvement of new corrosion mechanisms when increasing the reactor power, and may necessitate making corrections to the requirements for the water-chemistry regime (WCR) of the primary coolant for operation at the elevated power level. The point is that the conclusion about the absence of water chemistry upsets pertains to integral parameters of the coolant quality, but the coolant water chemistry may change locally, only in a certain area, such as the area where the white deposit is observed, while integrally remaining within the specified requirements throughout the entire circuit. The radiolysis suppression conditions may also change locally in this case.

"Radiolysis suppression"

End (stable) products of radiolysis include the following three substances: hydrogen H_2, oxygen O_2, and hydrogen peroxide H_2O_2. It should be emphasized that oxygen O_2, which is important in terms of corrosion problems, is not the primary product of radiolysis. It is formed at the final stage of the chain of electrochemical transformations. Molecular hydrogen captures radicals which may serve as precursors of molecular oxygen O_2.

Therefore, the initial concentration of H_2 also determines equilibrium concentrations of hydrogen itself and of H_2O_2 and O_2, i.e. the ratio of equilibrium concentrations of all three radiolysis products. As a result of presaturation of the circuit water by hydrogen, equilibrium concentrations of H_2O_2 and O_2 tend to zero after the reactor has reached full capacity.

This is precisely the phenomenon called "radiolysis suppression". Therefore, it is hydrogen content that plays the role of one of the key factors influencing the corrosion processes.
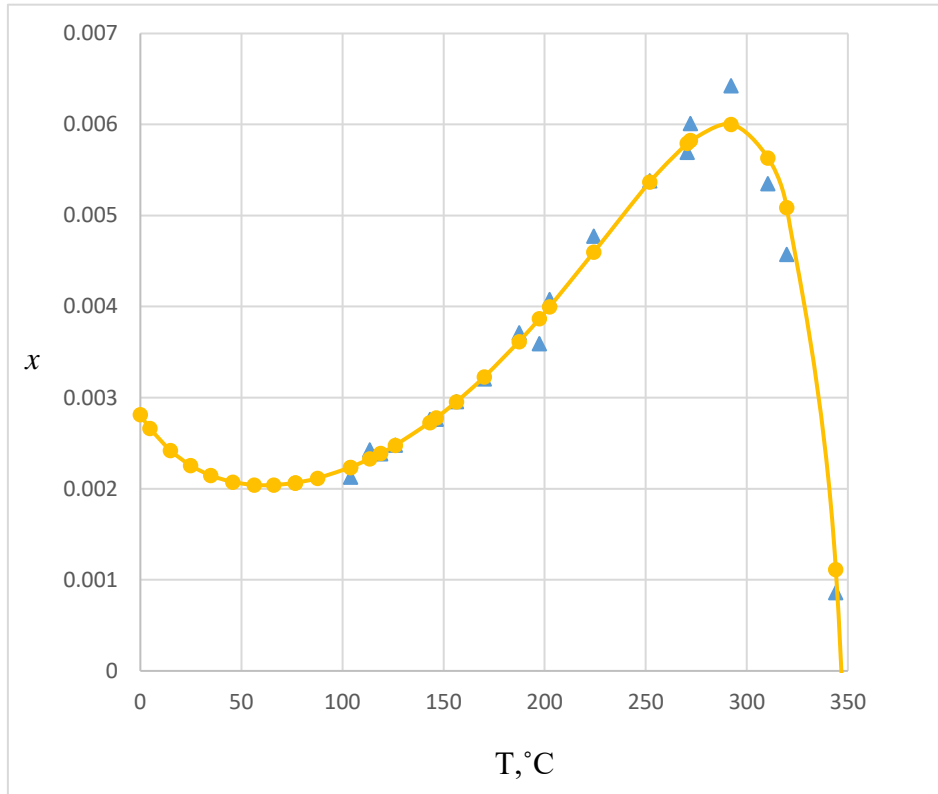
Solubility of hydrogen in water

Figure 2 – The solubility curve. Mole fraction of hydrogen x as function of temperature for pressure P=16 MPa

While approaching the temperature at which the solubility curve crosses the T-axis, the release of hydrogen shall intensify, and after passing through this point the solubility goes to zero. It should be noted that hydrogen shall be in thermodynamic equilibrium in the gas phase only. Thus, in the coolant boiling region there is observed a pronounced tendency to hydrogen depletion in the coolant and drastic change of water-chemistry regime parameters. The hydrogen concentration reduction value is determined both by kinetics of the gas phase bubbles nucleation and growth and by kinetics of hydrogen release to bubbles.

Diffusion of dissolved hydrogen into formed bubbles

Now we proceed to the consideration of the problem of gas diffusion into a bubble with a moving phase boundary in a bounded spherical domain of radius S (see Figure 3). For the diffusion mode, the bubble growth dynamics can be described by the following differential equation:
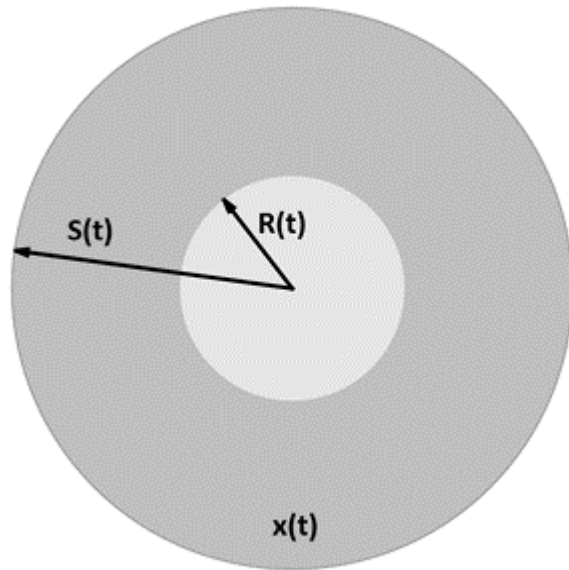
$$\frac{\partial n(r,t)}{\partial t} = D\Delta n(r,t) - div\left[n(r,t)\vec{v}(\vec{r},t)\right],$$

$$v_r(r,t) = \frac{R^2(t)}{r^2}\frac{dR(t)}{dt},$$

$$n(r,0) = n_0, r \in [R_0, S_0],$$

$$\left(\frac{dn}{dr}\right)_{r=S} = 0; t \geq 0,$$

the Henry's law: $x(R,t) = \frac{P_{H_2}}{k_H}; t \geq 0$, $P_{H_2} = n_{H_2}kT.$

The partial pressure of hydrogen in the bubble $P_{H_2} = P - P_{H_2O} + 2\sigma/R$, where σ is the water surface tension coefficient. The increase in the amount of hydrogen in a bubble increases its radius.

Figure 3 – Schematic representation of the liquid–bubble system at time t
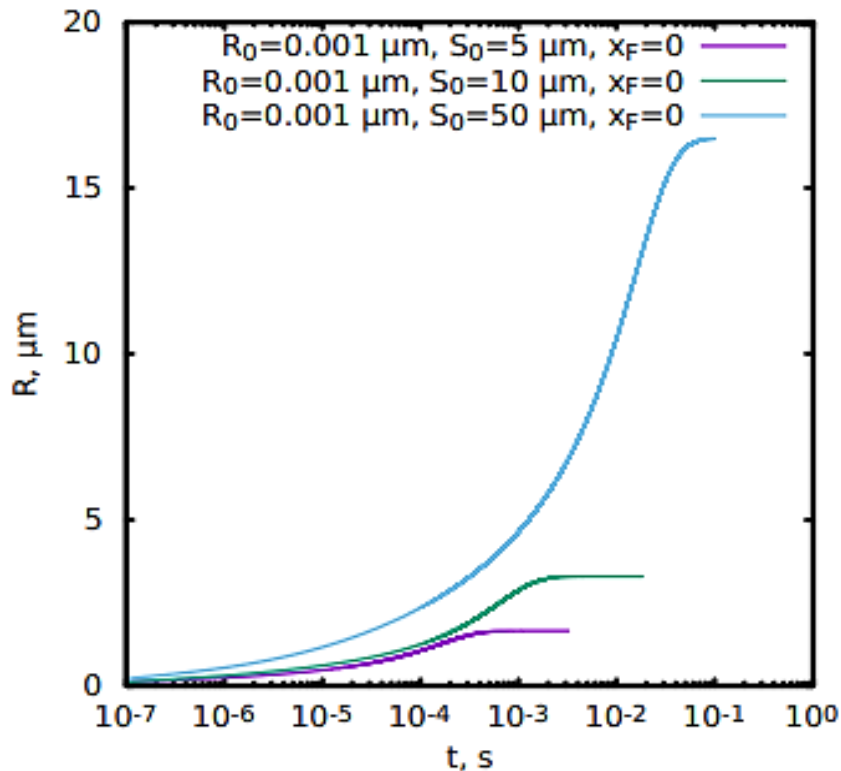
Results of numerical calculations

Figure 4 – Bubble radius versus time for three cases of the initial domain radius S_o in the case of complete release of hydrogen

System of equations was solved numerically. Results of numerical calculations were obtained for parameters corresponding to the reactor conditions.

According to the obtained data, the hydrogen content of the coolant may reduce by several orders of magnitude during time $\tau \sim 10^{-3}$ s or $\sim 10^{-1}$ s depending on the concentration of bubbles. In actual situations, however, the minimum concentration of critical nuclei in the reactor coolant at conditions under consideration according to our estimates is close to 10^{11} cm^{-3}. This corresponds to $S_o \sim 5$ µm, and thus the characteristic time of the hydrogen solution decomposition will be $\sim 5 \cdot 10^{-4}$ s.
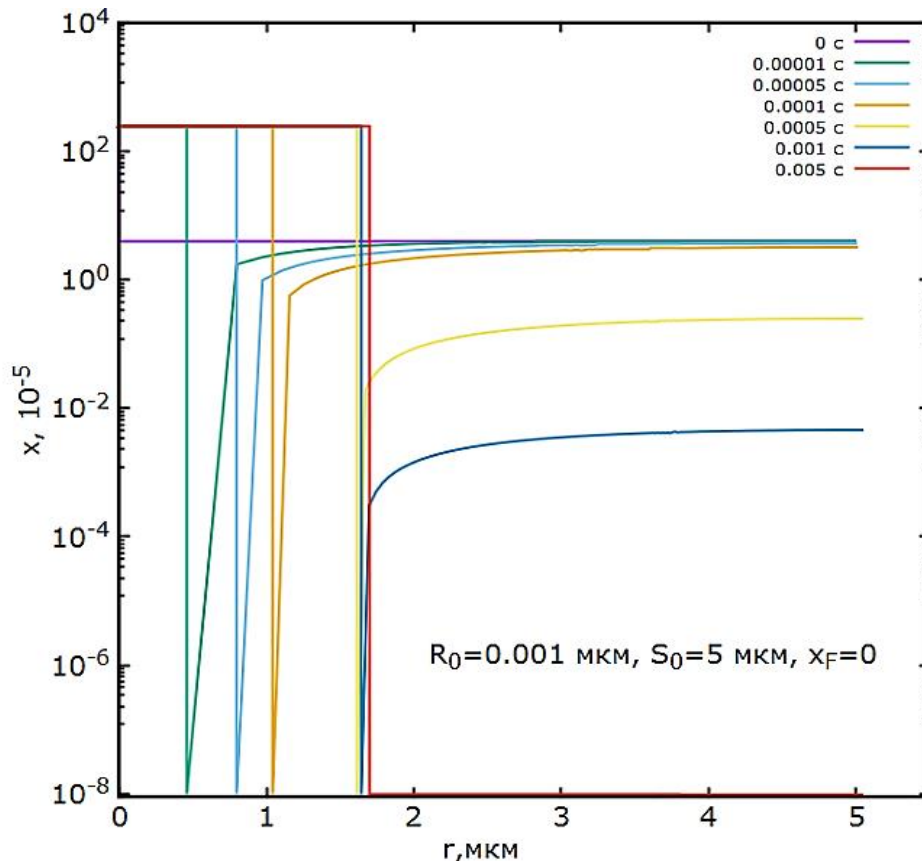
Evolution of the concentration profiles

Figure 5 – Evolution of concentration profiles for in the case of exit from the zone of absence of solubility.

Figure 5 show the evolution of the hydrogen concentration profiles for the hydrogen release from the bubble.

The times corresponding to different concentration profiles are shown in the upper right corner of each figure in seconds.

According to the presented data, the hydrogen content of the coolant may reduce by orders of magnitude during time $\tau \sim 10^{-3}$ s or $\sim 10^{-1}$ s depending on the domain radius S_o. In the majority of cases the kinetics of hydrogen release into bubbles is very fast and corresponds to the domain radius S_o of ~ 5 µm.

Mathematical modeling of radiolysis

According to the contemporary view, the process of radiolysis can be broken down into two stages: a fast stage of reactions near tracks of charged particles, and a relatively slow stage of chemical interaction between the radiolysis products within the volume of the medium. The mathematical modeling of the radiolysis process relates mostly to its second stage, The kinetic model of the second stage of radiolysis, which describes the time variation of concentrations of radiolysis products, represents a system on nonlinear differential equations of the following form:

$$\frac{dc_i}{dt} = \left(J_\gamma G_i^\gamma + J_n G_i^n + J_\alpha G_i^\alpha \right) + \sum_{p,q} k_{pq} c_p \, c_q - \sum_r k_{ir} \, c_i c_r$$

Here c_i, c_p, c_q, c_r are concentrations of particles of kinds i, p, q, r, k_{pq} and k_{ir} are constants of the rate of generation and annihilation of particles of kind i, respectively, in reactions between particles p, q and r.

The custom-developed code testing

A computer code was developed to solve the radiolysis problem.To make it more convincing, the developed code was further tested against standard results of computer modeling of radiolysis of pure water at high temperatures. The test results are presented in Figure 6.
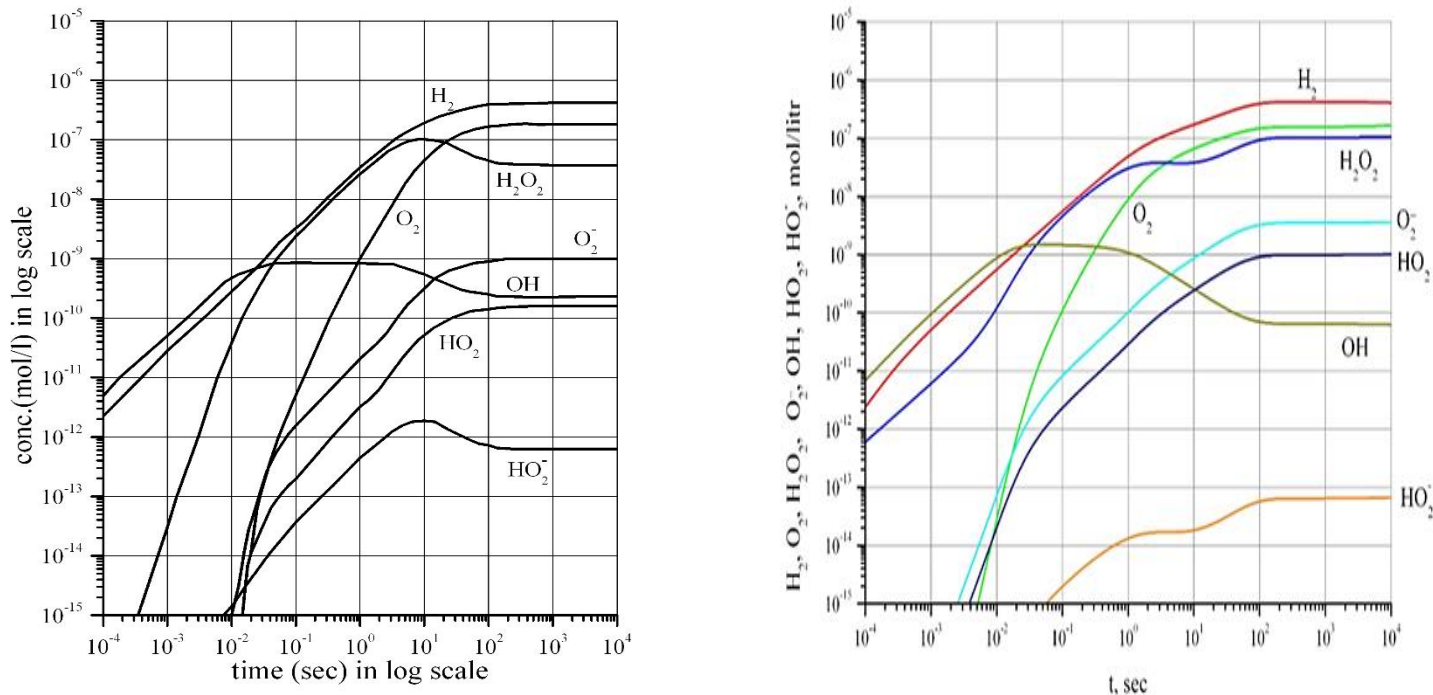

Figure 6 – Radiolysis of pure water at 250 °C, γ-radiation dose rate 4.5·10^4 rad/h. Left – standard result of computer modeling [*]; Right – calculation with the code we developed

[*] R. Sunaryo, Y. Katsumara and K Ishigure, "Radiolysis of water at elevated temperatures", Radiat. Phys. Chem. 45, 703-314, 1995.

The numerical solution of the system of kinetic equations for the VVER-1000 reactor conditions

The numerical solution of the system of kinetic equations for the VVER-1000 reactor conditions is presented in Figure 7. The figure shows the behavior of 11 components formed in water irradiated by neutrons and γ-quanta.
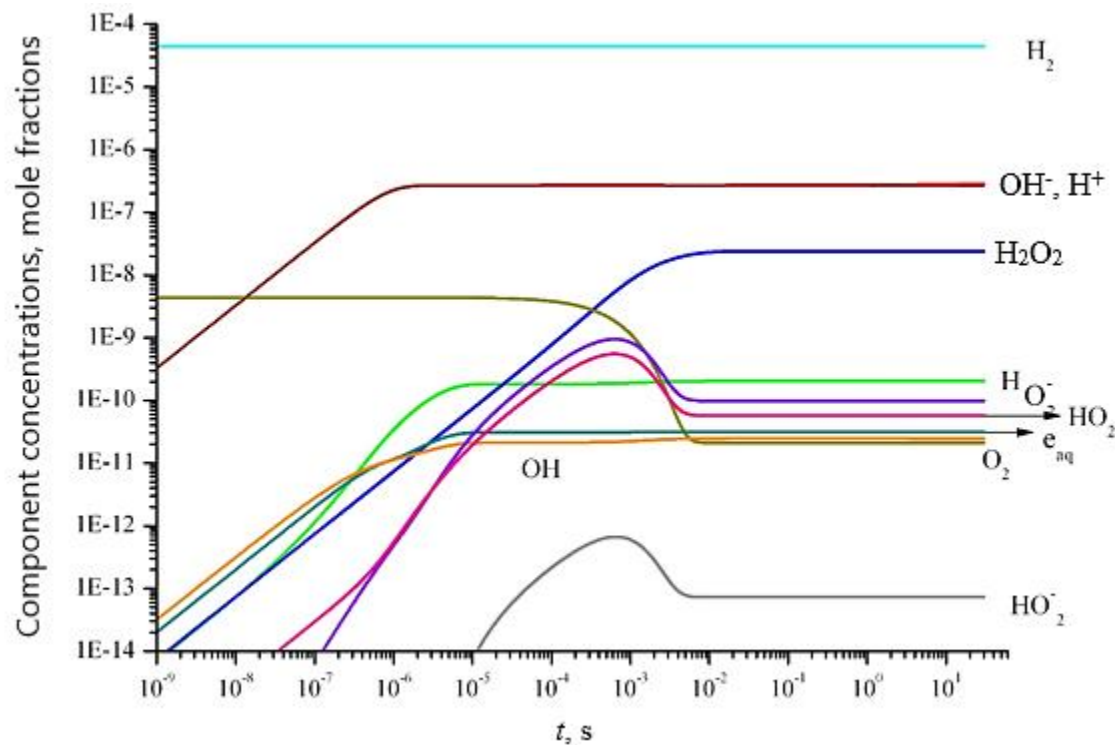

Figure 7 – Evolution of eleven relative concentrations of components in the water solution

Jointly solve the diffusion and the radiolysis problems

To estimate the change in the concentrations of H_2O_2 and O_2 with a sharp decrease in the concentration of hydrogen in the liquid phase, it is necessary to jointly solve the diffusion and the radiolysis problems. In the neighborhood of the saturation temperature the hydrogen concentration in the coolant changes very quickly, almost stepwise. This allows introducing the stepwise change in the hydrogen concentration into the system of equations (1) by means of the Heaviside function

$$\frac{dc_i}{dt} = \left(J_\gamma G_i^\gamma + J_n G_i^n + J_\alpha G_i^\alpha\right) + \sum_{p,q} k_{pq} c_p c_q - \sum_r k_{ir} c_i c_r - \chi c_m \delta_{im} \theta(t - t_0),$$

where subscript *m* refers to molecular hydrogen; $\theta(t - t_0)$ is the Heaviside function:

$$\theta(t - t_0) = \begin{cases} 0, & t < t_0; \\ 1, & t \geq t_0. \end{cases}$$

χ = 1/τ, τ is the chracterstic time of hydrogen release into bubbles; t_0 is the time when the jump in the hydrogen release starts; and δ_{im} is the Kronecker's symbol. The value of $t_0 = 5 \cdot 10^{-1}$ s mostly closely approaches the actual situation that is currently observed.

Release of hydrogen into bubbles. Calculation of radiolysis in water

The solution of the system of kinetic equations (6) of radiolysis of the water solution for the case of complete release of hydrogen into bubbles is shown in the figure 8.
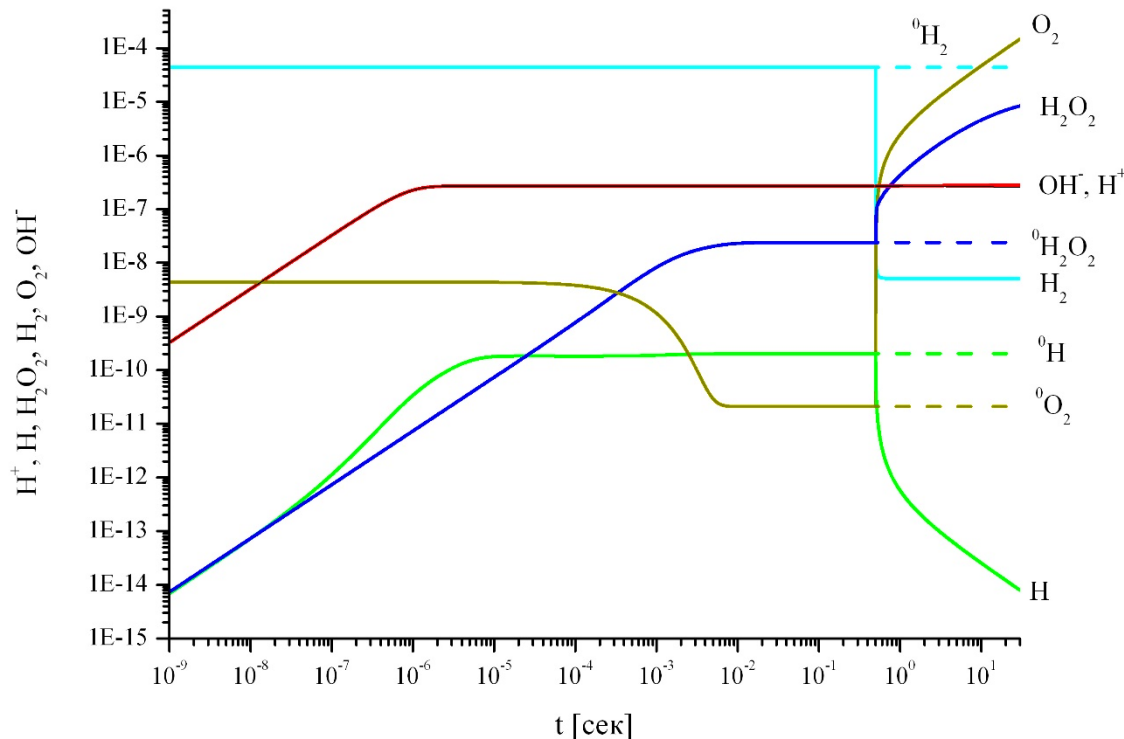

Figure 8 – Radiolysis of the water solution with $H_2 - 4.4 \cdot 10^{-5}$; $O_2 - 4.4 \cdot 10^{-9}$. Parameters of the H_2 jump: $t_0 = 0.5$ s; $\tau = 5 \cdot 10^{-4}$ s

According to Figure 8, the jump of the hydrogen concentration involves a drastic change in the entirety of time dependences of the component concentrations. This is especially true of concentration behavior of O_2 and H_2O_2, which are main oxidizers of zirconium claddings of fuel elements. By the time of 1 s, the mole fraction of oxygen jumps up by five orders of magnitude to ~ $5 \cdot 10^{-6}$. Hydrogen peroxide H_2O_2 demonstrates similar behavior. Its concentration increases greater than an order of magnitude.

Conclusion

The detailed study of the process of hydrogen release into gas-vapor bubbles near the coolant saturation temperature has shown that the concentration of hydrogen in the coolant may be reduced by several orders of magnitude during a very short time.

In this case, the coolant may in some zones deviate from the strict water-chemistry regime aimed to suppress radiolysis. In this case the efficiency of radiolytic oxygen suppression reduces drastically, and concentration of the radiolytic oxygen and hydrogen peroxide in the coolant may increase considerably, thus promoting local oxidation of fuel element claddings.

The significant local increase in the concentration of oxidizing radiolysis products – O_2 and H_2O_2 – in the coolant appears to be the main reason for formation of white deposit on VVER fuel element claddings in the vicinity of the 12th SG when increasing the reactor power.

NRC "Kurchatov Institute"

E-mail: asi.kiae@gmail.com;
Ivanov_AS@nrcki.ru

Thank you for your attention!